3108 *Chem. Mater.* **2010,** *22,* 3108–3113
DOI:10.1021/cm100086x

CHEMISTRY OF MATERIALS
Article

Morphology Dependence of Silicon Nanowire/ Poly(3,4-ethylenedioxythiophene):Poly(styrenesulfonate) Heterojunction Solar Cells

Shu-Chia Shiu, Jiun-Jie Chao, Shih-Che Hung, Chin-Liang Yeh, and Ching-Fuh Lin*

Graduate Institute of Photonics and Optoelectronics, National Taiwan University, Taipei, Taiwan 10617 R.O.C.

Received January 11, 2010. Revised Manuscript Received April 11, 2010

The characteristics of well-aligned silicon nanowire (SiNW)/poly(3,4-ethylenedioxy- thiophene): poly(styrenesulfonate) (PEDOT) heterojunction solar cells with varying nanowire lengths are investigated. PEDOT adheres on the hydrophilic *n*-type silicon nanowire surface to form a core−sheath heterojunction structure through the solution process. Such a structure increases the area of heterojunctions and shortens the carrier diffusion distance, and therefore, it greatly increases carrier collection efficiency. The cells exhibit stable rectifying diode behavior. Compared to the cells without a nanowire structure, the series resistance of the SiNW/PEDOT cell decreases from 60.42 Ω cm^2 to 1.47 Ω cm^2, and the power conversion efficiency improves from 0.08% to 5.09%. The SiNW/ PEDOT solar cell harvests photons from 400 nm to 1100 nm and a maximum incident photocurrent conversion efficiency of ∼32% at 700 nm.

Introduction

The polymer/semiconductor heterojunction attract lots of attention to solar cells because of several advantages, including large-area coverage, low-temperature process capability, easy preparation, low cost, and so on. To date, researchers have demonstrated planar polymer/ semiconductor heterojunction solar cells based on crystalline or amorphous silicon such as poly-$(CH_3)_3$Si-cyclooctatetraene/n-Si,[1] tetraphenylporphyrin/n-Si,[2] 4-tricyanovinyl-*N*,*N*-diethylaniline/p-Si,[3] poly(3-hexylthiophene)/ a-Si,[4] poly(3,4-ethylenedioxy thiophene):poly(styrenesulfonate)/n-Si,[5] polyaniline/n-Si,[6] and phthalocyanine/ n-Si,[7] etc. However, with a planar polymer/silicon cell structure, only the photogenerated electron−hole pairs (EHPs) near the junction will be separated and collected into electrical contacts. Other photogenerated EHPs produced in the polymer and the silicon mostly will be lost as a result of recombination. This limits the power conversion efficiency (PCE) of the polymer/silicon heterojunction solar cells.

To improve the EHP separation and collection, the use of SiNW structures in solar cells is a promising direction because of the enormous increase of the p-n junction area and the short carrier diffusion distance.[8−12] In addition, the nanowire structure can significantly reduce reflection[13−15] and induce strong light trapping between nanowires,[16−18] resulting in strong absorption. Mostly, to form SiNW p-n junction structures, a thin amorphous or nanocrystal silicon layer was deposited on the SiNW surface by chemical vapor deposition.[8,11] The cells show a

*Corresponding author. Graduate Institute of Photonics and Optoelectronics, Graduate Institute of Electronics Engineering and Department of Electrical Engineering, National Taiwan University, Taipei 10617, Taiwan, ROC. Tel: +886 2 3366 3540. Fax: +886 2 2364 2603. E-mail: cflin@cc.ee.ntu.edu.tw.

(1) Sailor, M. J.; Ginaburg, E. J.; Gorman, C. B.; Kumar, A.; Grubbs, R. H.; Lewis, N. S. *Science* **1990**, *249*, 1146–1149.
(2) El-Nahass, M. M.; Zeyada, H. M.; Aziz, M. S.; Makhlouf, M. M. *Thin Solid Films* **2005**, *492*, 290–297.
(3) El-Nahass, M. M.; Zeyada, H. M.; Abd-El-Rahman, K. F.; Darwish, A. A. A. *Sol. Energy Mater. Sol. Cells* **2007**, *91*, 1120–1126.
(4) Gowrishankar, V.; Scully, S. R.; McGehee, M. D.; Wang, Q.; Branz, H. M. *Appl. Phys. Lett.* **2006**, *89*, 252102.
(5) Williams, E. L.; Jabbour, G. E.; Wang, Q.; Shaheen, S. E.; Ginley, D. S.; Schiff, E. A. *Appl. Phys. Lett.* **2005**, *87*, 223504.
(6) Wang, W.; Schiff, E. A. *Appl. Phys. Lett.* **2007**, *91*, 133504.
(7) Lin, C. H.; Tseng, S. C.; Liu, Y. K.; Tai, Y.; Chattopadhyay, S.; Lin, C. F.; Lee, J. H.; Hwang, J. S.; Hsu, Y. Y.; Chen, L. C.; Chen, W. C.; Chen, K. H. *Appl. Phys. Lett.* **2008**, *92*, 233302.
(8) Tsakalakos, L.; Balch, J.; Fronheiser, J.; Korevaar, B. A.; Sulima, O.; Rand, J. *Appl. Phys. Lett.* **2007**, *91*, 233117.
(9) Maiolo, J. R., III; Kayes, B. M.; Filler, M. A.; Putnam, C. P.; Kelzenberg, M. D.; Atwater, H. A.; Lewis, N. S. *J. Am. Chem. Soc.* **2007**, *129*, 12346–12347.
(10) Goodey, A. P.; Eichfeld, S. M.; Lew, K. K.; Redwing, J. M.; Mallouk, T. E. *J. Am. Chem. Soc.* **2007**, *129*, 12344–12345.
(11) Garnett, E. C.; Yang, P. *J. Am. Chem. Soc.* **2008**, *130*, 9224–9225.
(12) Huang, J. S.; Hsiao, C. Y.; Syu, S. J.; Chao, J. J.; Lin, C. F. *Sol. Energy Mater. Sol. Cells* **2009**, *93*, 621–624.
(13) Hu, L.; Chen, G. *Nano Lett.* **2007**, *7*, 3249–3252.
(14) Huang, Y. F.; Chattopadhyay, S.; Jen, Y. J.; Peng, C. Y.; Liu, T. A.; Hsu, Y. K.; Pan, C. L.; Lo, H. C.; Hsu, C. H.; Chang, Y. H.; Lee, C. S.; Chen, K. H.; Chen, L. C. *Nat. Nanotechnol.* **2007**, *2*, 770–774.
(15) Sivakov, V.; Andra, G.; Gawlik, A.; Berger, A.; Plentz, J.; Falk, F.; Christiansen, S. H. *Nano Lett.* **2009**, *9*, 1549–1554.
(16) Tsakalakos, L.; Balch, J.; Fronheiser, J.; Shih, M. Y.; LeBoeuf, S. F.; Pietrzykowski, M.; Codella, P. J.; Korevaar, B. A.; Sulima, O.; Rand, J.; Davuluru, A.; Rapol, U. *J. Nanophoton.* **2007**, *1*, 013552.
(17) Muskens, O. L.; Rivas, J. G.; Algra, R. E.; Bakkers, E. P. A. M.; Lagendijk, A. *Nano Lett.* **2008**, *8*, 2638–2645.
(18) Muskens, O. L.; Diedenhofen, S. L.; Kaas, B. C.; Algra, R. E.; Bakkers, E. P. A. M.; Rivas, J. G.; Lagendijk, A. *Nano Lett.* **2009**, *9*, 930–934.

Published on Web 04/26/2010

spectrally broad incident phototo-current conversion efficiency (IPCE) in the visible region but low IPCE in the near-infrared region.[8] High series and low shunt resistances appear to limit the PCE of these cells to below 1%. In this work, the hole-conducting polymer poly(3,4-ethylenedioxythiophene):poly(styrenesulfonate) (PEDOT:PSS) is coated on the SiNWs to replace the p-doped amorphous or nanocrystal silicon layer. The highest occupied molecular orbital (HOMO) energy of PEDOT is ~5.1 eV,[19] which is similar to the valence band energy of silicon. Thus, the interface between the PEDOT layer and n-type SiNWs could possibly form good heterojunctions for EHPs separation. In addition, a planar front transparent conductive layer is used to contact the top of every SiNW via PEDOT instead of conventional metal fingers. Thus, it greatly shortens the carrier transport distance. Our investigation shows that the current-to-voltage (J-V) characteristics of the SiNW/PEDOT cells clearly reveal stable rectifying diode behavior. In addition, the SiNW/PEDOT structure could greatly improve the separation and collection of the EHPs and induce a light trapping effect, leading to enhanced IPCE in the near-infrared region. The PCE is also greatly improved in the SiNW/PEDOT cells as compared to the cells without a nanowire structure.

Experimental Section

Fabrication of SiNWs Arrays. SiNWs were made by an aqueous electroless etching method.[20] An n-type 1−10 Ω-cm Si (100) wafer was used to synthesize SiNWs in an aqueous solution of $AgNO_3$ and HF acid at room temperature. The solution concentration of $AgNO_3$ and HF was 0.023 and 5.6 mol L^{-1}, respectively. After etching, the arrays of SiNWs were immersed in a concentrated nitric acid bath to remove all Ag dentritic structures from the nanowire surfaces. Finally, the SiNWs were immersed in the BOE to remove the oxide layer on the SiNWs and form H-terminated bonds on the silicon surface. SiNW arrays prepared by this method are aligned vertically over the area up to the wafer size. The aluminum was evaporated on the silicon back side as the electrical contact.

SiNW Solar Cell Fabrication. The poly(3,4-ethylenedioxythiophene):poly(styrenesulfonate) (Baytron P, H. C. Starck GmbH, Leverkusen, Germany) was used to form SiNW/PEDOT heterojunctions. The PEDOT gel particles with a mean diameter of 80 nm were dispersed in the aqueous solution. However, the SiNW surface with H-terminated bonds exhibited a hydrophobic effect after being immersed in the BOE. To form SiNW/PEDOT heterojunction structures, the SiNW surface should be modified to become a hydrophilic surface. This could make PEDOT adhere to the SiNW surface. To form a hydrophilic surface, the SiNWs were put in an environment with a relative humidity of 60% and 25 °C for 2 h to form a very thin native oxide layer on the SiNW surface. A silicon surface with a thin native oxide is hydrophilic and has a contact angle below 20°. Then, the PEDOT was spin-coated on the ITO-coated glass instead of being directly spin-coated on the SiNW arrays. The thickness of the wet PEDOT film was 9 μm (the thickness of the dry film was 200 nm). Before the PEDOT thin film dried, the top portion of the SiNWs was immersed in the wet PEDOT thin film. Figure 1 shows schematic diagrams describing the procedures for fabricating SiNW/PEDOT core−sheath heterojunction solar cells. The SiNWs fabricated by metal-assisted etching are vertically aligned and are very uniform in length. Therefore, almost all SiNWs can be immersed in the wet PEDOT thin film. Afterward, the samples were annealed at 140 °C for 10 min in an N_2 environment. The wet PEDOT was dried and formed a compact film on the SiNWs surface. Then, each individual SiNW was stuck on an ITO electrode via PEDOT. The solution process gives solar cells a cost benefit in comparison with the use of chemical vapor deposition.

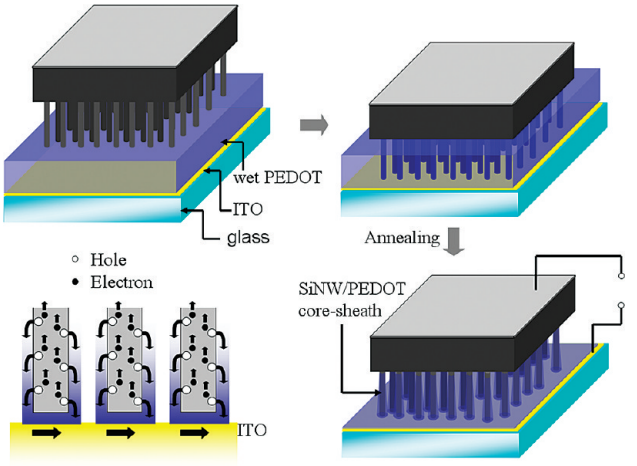

Figure 1. Schematic diagrams describing the procedures for fabricating SiNW/PEDOT core−sheath heterojunction solar cells.

Characterization. To characterize the SiNW/PEDOT structure, scanning electron microscopy (SEM) imaging was performed with an Elionix ERA-8800 microscope. In addition, transmission electron microscopy (TEM) images were taken with a Philips Tecnai F30 microscope system. The J-V characteristics were measured by using a Keithley 2400 electrometer in air-in-dark conditions. To measure the photovoltaic J-V characteristics, a solar simulator (SUN 2000, Abet Technologies, Inc.) was used as a light source. The incident light falls normally through the glass substrate and ITO on the SiNW/PEDOT heterojunction structure with an intensity 100 mW/cm^2 under air mass 1.5 conditions. To investigate the contact between the SiNWs and the ITO, the 2-D photocurrent mapping for the SiNW/PEDOT cell was measured by using a 632 nm He−Ne laser. The incident phototo-current conversion efficiency (IPCE) spectra were measured using a tungsten−halogen lamp in combination with a monochromator. The input light was modulated with a mechanical chopper. Then the response was recorded by a lock-in amplifier. A calibrated Si cell was used as a reference.

Results and Discussion

Figures 2a shows the side-view SEM images of the as-etched SiNWs, which are vertically aligned on the silicon substrate. Figure 2b shows the top-view SEM image of the as-etched SiNWs. The distribution of nanowire sizes ranges from 20 to 289 nm. Figure 2c shows the side-view SEM image of the SiNWs detached from ITO coated glass by a mechanical force. The SiNWs detached from ITO coated glass reveals that the PEDOT layer is covered

(19) Girotto, E. M.; Gazotti, W. A.; De Paoli, M. A. *J. Phys. Chem. B* **2000**, *104*, 6124–6127.
(20) Peng, K.; Hu, J.; Yan, Y.; Wu, Y.; Fang, H.; Xu, Y.; Lee, S.; Zhu, J. *Adv. Funct. Mater.* **2006**, *16*, 387–394.

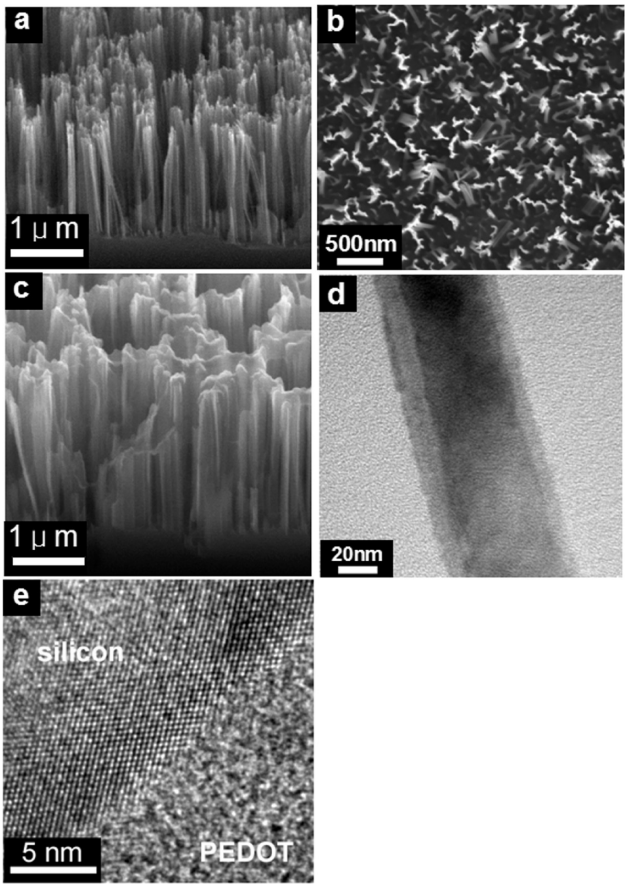

Figure 2. (a) Side-view SEM image of the as-etched SiNWs. (b) Top-view SEM image of the as-etched SiNWs. (c) SEM image of the SiNWs covered with the PEDOT thin film layer. (d) TEM image of the SiNW/PEDOT core−sheath structure. (e) TEM image of the SiNW/PEDOT interface.

on the SiNWs. To further investigate the SiNW/PEDOT structures, the TEM image of the SiNWs detached from ITO coated glass is showed in Figure 2d. The single crystalline core is aligned to a zone axis, leading to much stronger diffraction and thus darker contrast compared to that of the PEDOT sheath. The thickness of the PEDOT is below 20 nm. This can confirm that the PEDOT covers the surface of the SiNWs but does not cover just the top of the SiNWs. The high-resolution TEM image taken near the edge of the SiNW (Figure 2e) reveals that the PEDOT compactly adhered on the SiNW surface.

The formation of the thin PEDOT sheath on the SiNW surface can be explained by the following mechanism. First, the PEDOT gel particles with a mean diameter of 80 nm adhered on the SiNW surface when the SiNWs were immersed in the wet PEDOT film. Hydrogen bonds developed between HSO_3 groups of the PSS-rich outer shell of individual PEDOT gel particles connected to individual PEDOT gel particles.[21] A wet PEDOT film formed on the SiNW surface. Because the space between the SiNWs is about 100 nm−200 nm, a few layers of PEDOT gel particles can stack on the SiNW surface. Then, the water in the gel particles evaporated during the

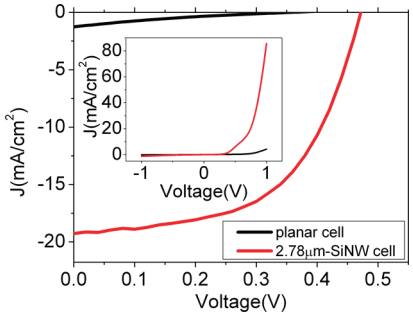

Figure 3. Light (under simulated AM1.5 conditions) current−voltage characteristics of the SiNW/PEDOT cell and the planar cell. The inset shows the dark current−voltage characteristics.

annealing process. This process caused some lateral shrinkage of PEDOT gel particles and a considerable decrease in thickness took place. Finally, a PEDOT thin film formed on the SiNW surface. Recent reports have indicated that the PEDOT gel particles will form lamellar particles after drying, which had a diameter of 20−25 nm and a thickness of 5−6 nm.[21,22] The stacks of the lamellar particles formed a pancake-like morphology. The PEDOT film with a few layers of PEDOT lamellar particles formed a thin sheath with a thickness of about 20 nm on the SiNW surface.

The photovoltaic J-V characteristic of the SiNW/PEDOT solar cell was measured under an illumination intensity of 100mW/cm^2 (AM1.5G). A strong increase in short-circuit current density (J_{sc}), open-circuit voltage (V_{oc}), fill factor (*FF*), and PCE was observed in the cells with 2.78-μm SiNW structures (Figure 3), as compared to the planar cell without nanowires. The J_{sc} is improved from 1.27 mA/cm^2 to 19.28 mA/cm^2, the V_{oc} from 0.34 to 0.47 V, and the *FF* from 18% to 61%, resulting in an improvement of the PCE from 0.08% to 5.09%. The increase of the short circuit current is due to two major reasons. First, the carrier diffusion distance from the core of the SiNW to SiNW/PEDOT heterojunction is only several tens of nanometers or below. The distance may be several micrometers in the planar cells. Thus, the EHP separation and collection efficiency is greatly enhanced in the SiNW/PEDOT cells. Second, the reflectance of the SiNW arrays reduces to below 5% over the spectral range of 400−1100 nm as compared to the planar silicon surface with reflectance of over 30%. In addition, light trapping in the SiNW arrays increases the absorption of SiNWs. These lead to the enhancement of the photocurrent.

In the inset of Figure 3, the dark current density at a forward bias also was enhanced in the SiNW/PEDOT cell, as compared to the planar cell. The measured current-to-voltage (J-V) characteristics of the SiNW/PEDOT cells clearly reveal a stable rectifying diode behavior. The series resistance decreases from 60.42 Ω cm^2 for the planar cell to 1.47 Ω cm^2 for the SiNW/PEDOT device. The improvement in the fill factor for the SiNW/PEDOT

(21) Lang, U.; Muller, E.; Naujoks, N.; Dual, J. *Adv. Funct. Mater.* **2009**, *19*, 1215–1220.
(22) Nardes, A. M.; Kemerink, M.; Janssen, R. A. J.; Bastiaansen, J. A. M.; Kiggen, N. M. M.; Langeveld, B. M. W.; van Breemen, A. J. J. M.; de Kok, M. M. *Adv. Mater.* **2007**, *19*, 1196–1200.
(23) Dash, W. C.; Newman, R. *Phys. Rev.* **1955**, *99*, 1151–1155.

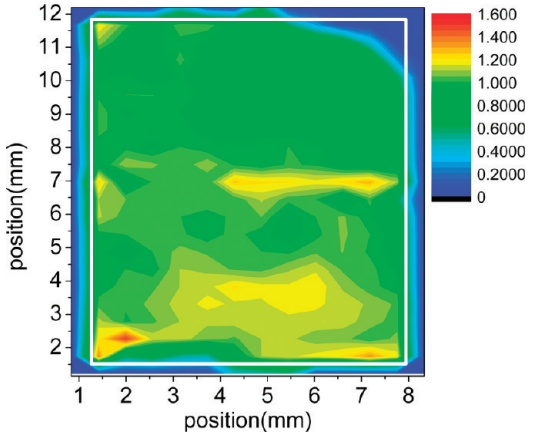

Figure 4. 2-D photocurrent mapping of the SiNW/PEDOT solar cell.

cells could be attributed to this general reduction in the series resistance. The result indicates that the SiNW structure increases the heterojunction area and thus greatly enhances current density. The series resistance of the SiNW/PEDOT heterojunction cells is even lower than that of SiNW homojunction cells reported in the literature.[8,11] The reason is that, in the architecture of the SiNW/PEDOT cells, the charge carriers can directly transport between the SiNW and the planar ITO electrode through PEDOT. Therefore, the reduction of the series resistance due to the increase in the junction area can be observed.

To investigate the uniformity of the SiNW/PEDOT heterojunction and the contact of the SiNWs on the ITO surface, 2-D photocurrent mapping was measured as shown in Figure 4. The white frame in Figure 4 indicates the active region of the SiNW/PEDOT solar cell. The results show that the photocurrent map has a uniform response within the active region. This means that most photogenerated EHPs in the SiNWs can be separated and collected in the electrical contacts. The holes are collected in the ITO film, and the electrons are collected in the aluminum contact. This experiment also indicates that most SiNWs can be stuck on the ITO electrode via PEDOT. The architecture of the cell takes advantage of charge carrier transport in the nanowire structures. A planar ITO thin film is used to contact the top of the SiNWs via PEDOT as front contacts instead of conventional metal fingers. In conventional planar solar cells, charge carriers in the emitter will transport near the front surface to the metal fingers. Therefore, if the front surface of the solar cells forms nanostructures, the charge carriers in the emitter will transport a much longer distance than that in the planar solar cells. This may increase the series resistance. The cell architecture proposed here means that the charge carriers separated in the SiNWs could be immediately collected to the ITO electrode instead of diffusing a long distance through SiNW arrays as shown in the illustration of Figure 1. It could lower the series resistance of SiNW solar cells.

To further investigate the reasons for the improved efficiency, the IPCE spectrum of the SiNW/PEDOT device was measured and shown in Figure 5a. The cell

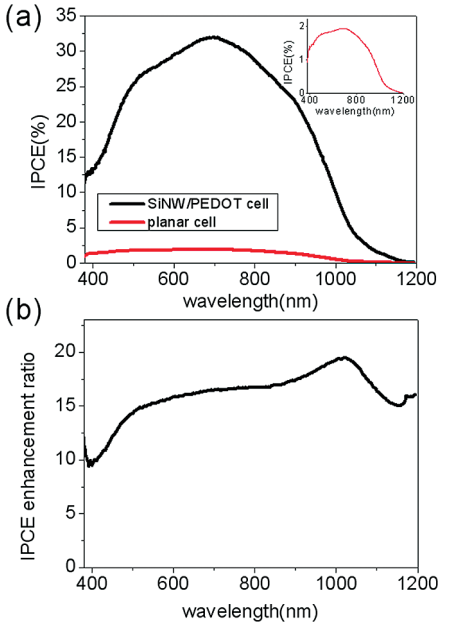

Figure 5. (a) IPCE spectra of the SiNW/PEDOT cell and the planar cell. The SiNW/PEDOT cell exhibits a maximum IPCE of ~32% at 700 nm. The inset shows the IPCE spectrum of the planar cell. (b) IPCE enhancement ratio of the SiNW/PEDOT cell and the planar cell.

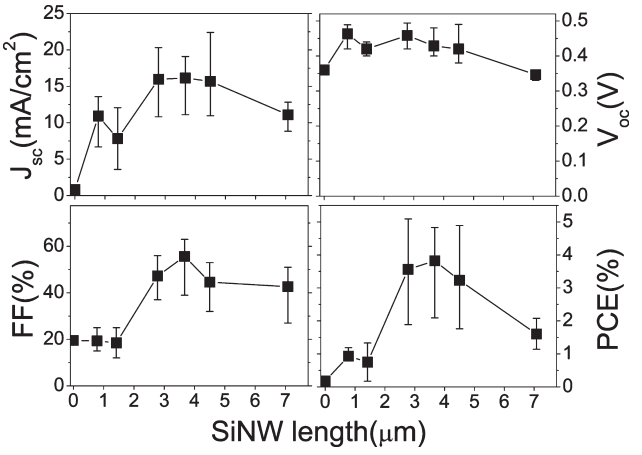

Figure 6. J_{sc}, V_{oc}, *FF*, and PCE of the SiNW/PEDOT cells are plotted as functions of the length of SiNWs.

harvests photons from 400 nm to 1100 nm and gives a maximum IPCE of 32% at 700 nm. In contrast, for planar cells, the maximum IPCE is only ~1.94% occurring at 682 nm, as shown in the inset of Figure 5a. The IPCE enhancement ratio is over 15 from 530 nm to 1100 nm as shown in Figure 5b. This ratio achieves a maximum value at the wavelength of 1014 nm. The phenomenon of the enhanced IPCE in the SiNW/PEDOT cell can be attributed to the light trapping effect. For the planar cell, light penetration depth in the silicon substrate is several micrometers in the visible region and several tens of micrometers in the NIR region.[23] The poor carrier collection efficiency in the deep region of the silicon substrate causes low photocurrent and low IPCE, especially in the NIR region. However, for the SiNW/PEDOT cell, the strong light trapping effect in the SiNW structure increases the optical absorption from the visible region to the NIR

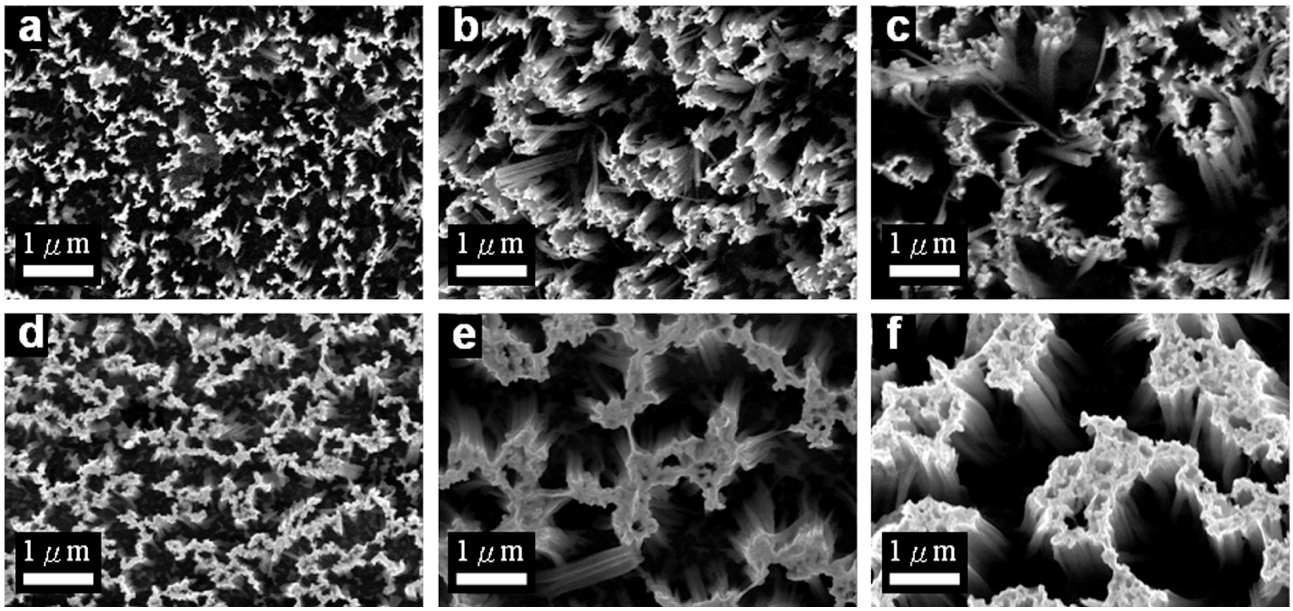

Figure 7. (a, b, and c) Top-view SEM images of the as-etched SiNWs with lengths of 2.78, 4.5, and 7.08 μm, respectively. (d, e, and f) SiNWs covered with PEDOT with lengths of 2.78, 4.5, and 7.08 μm, respectively.

region.[12,16] Furthermore, the core−sheath structure facilitates efficient EHP separation and collection in the radial directions of nanowires. Thus, the IPCE can be greatly enhanced.

The length of SiNWs also greatly influences the optical properties of SiNW arrays, including absorption and light-trapping between nanowires. A stronger light trapping effect induced in longer SiNW arrays is expected. A small ratio of light could penetrate through long SiNWs and be absorbed in the deep region of silicon substrates, while the greatest ratio of light is absorbed in SiNWs. Therefore, the PCE of cells could increase as the SiNW length increases. In Figure 6, the performance parameters of the SiNW/PEDOT cells (J_{sc}, V_{oc}, *FF*, and PCE) are plotted as functions of the SiNW length. For each length of SiNWs, several solar cells are fabricated and measured. The average values of the performance parameters for each SiNW length are plotted. As shown in Figure 6, the average J_{sc} in the SiNW/PEDOT cells increases from 10.9 mA/cm^2 to 16.1 mA/cm^2 as the length of SiNWs increases from 0.78 to 3.67 μm. The average *FF* increases from 19% to 55%. Thus, the average PCE increases from 0.93% to 3.82%. However, the average J_{sc} decreases from 16.1 to 11 mA/cm^2 as the SiNW length further increases from 3.67 to 7.08 μm. The average V_{oc} of devices decreases from 0.42 to 0.34 V. The average *FF* decreases from 55% to 44%. Therefore, the average PCE of the devices drops dramatically from 3.82% to 1.6%.

In order to understand the decrease of device performance, a top view of the SiNWs covered with PEDOT was measured by SEM after removing the ITO-coated glasses. Figure 7d, e, and f is the top-view SEM images of the SiNWs covered with PEDOT for wire lengths of 2.78, 4.5, and 7.08 μm, respectively. For comparison, Figure 7a, b, and c shows the as-etched SiNWs with lengths of 2.78, 4.5, and 7.08 μm, respectively. The top

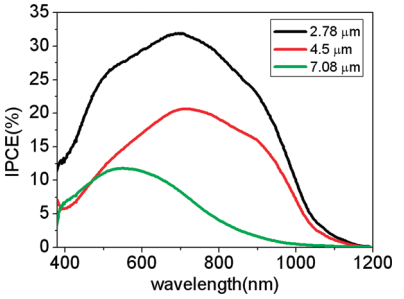

Figure 8. IPCE spectra of the SiNW/PEDOT cell with different lengths.

morphology of the SiNWs covered with PEDOT is strongly related to the wire length. As the wire length increases, the top portions of the SiNWs gradually aggregate and form large nanowire bundles, as shown in Figure 7f. The lateral size of the SiNW bundles is about 1−3 μm, which is much larger than the size of each individual SiNW. The bundle morphology is due to the surface tension of the PEDOT solution when the top portion of the SiNWs was immersed in the wet PEDOT thin film. The formation of large SiNW bundles leads to large hollow spaces between SiNW bundles.

The formation of large SiNW bundles influences the optical properties of the SiNW/PEDOT cells. The IPCE spectra of SiNWs with different lengths are shown in Figure 8. As the length of SiNWs increases from 2.78 to 4.5 μm, the IPCE decreases over a broad spectral range of 400−1100 nm. As the length of SiNWs increases to 7.08 μm, the IPCE further decreases over the spectral range of 400−1100 nm, especially at the NIR region. The result reveals that light penetrates the hollow spaces between SiNW bundles and then is absorbed by the deep region of the silicon substrate. The long diffusion distance of carriers from the Si substrate decreases the carrier collection efficiency and overall efficiency. Furthermore,

the absorption length of the light in the NIR region is longer than that in the visible region. Thus, the decrease of IPCE in the NIR region is more obvious than that in the visible region. This phenomenon can explain the fact that the increase of the SiNW length decreases the PCE of the SiNW/PEDOT solar cells.

Conclusions

The SiNW/PEDOT heterojunction solar cells were investigated. A high short-circuit current of 19.28 mA/cm^2 was found in SiNW/PEDOT heterojunction solar cells. The PCE of SiNW/PEDOT heterojunction solar cells achieves 5.09%, while the PCE of planar cells is only 0.08%. The SiNW/PEDOT cell gives a maximum IPCE of 32% at 700 nm. We also found that the morphology of SiNW bundles significantly influences the performance of the solar cells, making long SiNWs not necessarily beneficial to device performance. The techniques involved are simple and low-cost. The great improvement of PCE demonstrates that our approach could provide a possible route for the integration of organic and inorganic solar cells as well as various hybrid material systems.

Acknowledgment. We acknowledge the support of the National Science Council under contract numbers NSC 96-2221-E-002-277-MY3, NSC 97-2218-E-002-013, and NSC 97-2221-E-002-039-MY3.